Investigation of the Catalytic Mechanism of Farnesyl Pyrophosphate Synthase by Computer Simulation

Verónica Muriel Sanchez,[†] Alejandro Crespo,[†] J. Silvio Gutkind,[‡] and Adrián Gustavo Turjanski*[,†,‡]

Departamento de Química Inorgánica, Analítica y Química Física/INQUIMAE, Facultad de Ciencias Exactas y Naturales, Universidad de Buenos Aires/CONICET, Ciudad Universitaria, Pab. II, P. 3, C1428EHA Buenos Aires, Argentina, and Oral and Pharyngeal Cancer Branch, National Institute of Dental and Craniofacial Research, NIH, Bethesda, Maryland

Received: May 20, 2006; In Final Form: July 14, 2006

Farnesyl pyrophosphate synthase (FPPS) catalyses the formation of a key cellular intermediate in isoprenoid metabolic pathways, farnesyl pyrophosphate, by the sequential head-to-tail condensation of two molecules of isopentenyl diphosphate (IPP) with dimethylallyl diphosphate (DMAPP). Recently, FPPS has been shown to represent an important target for the treatment of parasitic diseases such as Chagas disease and African trypanosomiasis. Bisphosphonates, pyrophosphate analogues in which the oxygen bridge between the two phosphorus atoms has been replaced by a carbon substituted with different side chains, are able to inhibit the FPPS enzyme. Moreover, nitrogen-containing bisphosphonates have been proposed as carbocation transition state analogues of FPPS. On the basis of structural and kinetic data, different catalytic mechanisms have been proposed for FPPS. By analyzing different reaction coordinates we propose that the reaction occurs in one step through a carbocationic transition state and the subsequent transfer of a hydrogen atom from IPP to the pyrophosphate moiety of DMAPP. Moreover, we have analyzed the role of the active site amino acids on the activation barrier and the reaction mechanism. The structure of the active site is well conserved in the isoprenyl diphosphate synthase family; thus, our results are relevant for the understanding of this important class of enzymes and for the design of more potent and specific inhibitors for the treatment of parasitic diseases.

Introduction

Farnesyl diphosphate synthase (FPPS) is a key enzyme of the mevalonate pathway supplying sesquiterpene precursors for several classes of essential metabolites which are utilized for several biosynthetic pathways, namely, in the synthesis of squalene and sterols, dolichols, ubiquinone, prenylated proteins, and the isoprenoid side chain of heme a.[1] FPPS catalyzes the 1′−4 condensation of dimethylallyl pyrophosphate (DMAPP) with two molecules of isopentenyl pyrophosphate (IPP) to form FPP.[2]

Recently, bisphosphonates, an important class of drugs currently used to treat osteoporosis, Paget's disease, and hypercalcemia due to malignancy, have been found to have potent antiparasitic activity.[3−9] Several bisphosphonates were found to inhibit osteoclast-mediated bone resorption in vitro by inhibiting FPPS, thereby preventing protein prenylation in osteoclasts.[4,10,11] FPPS has also been identified as the molecular target of bisphosphonates in different parasites,[6,12−16] including both *Trypanosoma brucei*, the causative agent of African sleeping sickness, and *Trypanosoma cruzi*, the causative agent of Chagas' disease (CD), also called *American trypanosomiasis*. In Africa, sleeping sickness results in more than 500 000 diseases annually, and it is estimated that 16−18 million people worldwide are infected with CD; of those infected, 50 000 will die each year.[17] CD is the most important parasitic disease in Latin America in terms of its impact on national economies and public health systems.[18] Thus, there has been considerable interest in developing novel chemotherapeutic approaches, based on unique aspects of the physiology and metabolism of this parasite.

The structure of apo- and ligand-bound avian FPPS,[19,20] the structure of human FPPS,[21] and the structures of unliganded *Staphylococcus aureus* FPPS (FPPS-Sa), as well as two *Escherichia coli* FPPS (FPPS-Ec) ternary complexes have been determined.[8] One of these ternary complexes contains IPP and the noncleavable DMAPP analogue dimethylallyl *S*-thiolodiphosphate (DMSPP).[22] Recently, we have studied the structural characteristics of the *T. cruzi* FPPS (TcFPPS) by homology modeling and molecular dynamics,[23] and Gabelli et al. solved the structure by X-ray crystallography of the protein alone and in two complexes with substrates and inhibitors.[24] The catalytic site of the enzyme consists of a large central cavity formed by mostly antiparallel α-helices with two aspartate-rich regions (DDXX(XX)D) located on opposite walls. The aspartates mediate the binding of prenyl phosphates to the protein via bridging three Mg^{2+} ions.

On the basis of crystallographic and kinetic evidence, two types of mechanisms have been proposed,[8,19,24−27] those in which condensation is initiated by heterolytic cleavage of the carbon−oxygen bond of the allylic pyrophosphate, yielding a cationic intermediate, and those where the formation of the C_1–C_4 bond between the two substrates and rupture of the C_1–oxygen bond is simultaneous through a transition state (TS) with a carbocation

* To whom correspondence should be addressed. Phone: 01-301-402-7432. E-mail: turjanskia@mail.nih.gov.
† Universidad de Buenos Aires/CONICET.
‡ NIH.

10.1021/jp063099q CCC: $33.50
Published on Web 08/22/2006

SCHEME 1: Reaction Mechanism of FPPS[a]

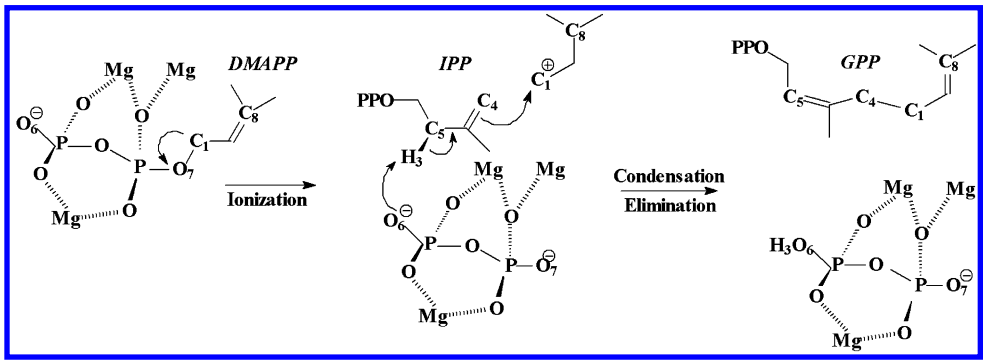

[a]The rupture of the C_1-O_7 bond of DMAPP leads to the generation of the transition state which has a carbocationic character. The subsequent formation of the C_1-C_4 bond occurs simultaneously with the hydrogen transfer from IPP to the pyrophosphate moiety of DMAPP, producing one molecule of GPP.

character (Scheme 1). Three conserved residues among different species, Thr[203], Gln[241], and Lys[202] have been proposed to stabilize the possible carbocation intermediate or TS.[8]

Although there is considerable structural information regarding FPPS, the mechanism of catalysis remains unclear. Modern modeling methods, including combined quantum mechanics and molecular mechanics (QM/MM) methods, can now give uniquely detailed understanding of enzyme-catalyzed reactions, as the analysis of mechanisms and the identification of determinants of specificity and catalytic efficiency.[28,29] In this sense, some recent applications to enzymes have proven the unique usefulness of this technique.[30−37] In this work we have studied the reaction mechanism catalyzed by FPPS using a QM/MM approach. We provide evidence that the reaction occurs in one step through the formation of a carbocationic transition state and the subsequent transfer of a hydrogen atom from IPP to the pyrophosphate moiety of DMAPP. Additionally, we have analyzed the role of key conserved amino acids in the reaction mechanism. The structural characteristics of the active site of FPPS are conserved throughout species, from bacteria to humans. Thus, our results are relevant for the understanding of this important class of enzymes and for the design of more potent and specific inhibitors for the treatment of parasitic diseases.

Materials and Methods

System Preparation. We have used the crystal structure of the protein FPPS from *E. coli* (PDB[38] code 1RQJ)[8] as the starting point for our calculations. The complex consists of FPPS−Ec, IPP, DMSPP, and three Mg^{2+} ions. DMSPP was changed to DMAPP. The system was solvated with TIP3P[39] water molecules up to a distance of 30 Å of the active center. The final system consisted of 6449 waters and 4647 protein atoms. All classical simulations were performed with the NAMD package[40] with the Amber force field[41] and the AMBER 8 package.[42] Partial charges for DMAPP and IPP were obtained using the restrained electrostatic fit (RESP) scheme.[43] Electrostatic potentials were computed using ab initio HF/6-31G** calculations using the Gaussian 98 package.[44] The parameters for DMAPP and IPP were taken from the AMBER force field.[41,45] The time step was 2 fs, the van der Waals interactions were smoothly cut off at 10 Å, and the Berendsen thermostat[46] was used to maintain the desired temperature. The complex structures were first equilibrated at 300 K for 100 ps keeping the whole protein fixed; as a restraint we used an harmonic potential with a force constant of 4 kcal/(mol·Å^2), to allow the water and the ligands molecules to relax. A subsequent 400 ps molecular dynamics without restraints was performed to allow the system to relax and equilibrate. Then the system was cooled slowly to 0 K.

QM/MM Methods. All QM computations were performed at the density functional theory (DFT) level with the SIESTA code.[47] DFT methods, including the SIESTA code, have shown an excellent performance for medium and large systems and have also proven to be appropriate for biomolecules.[30−33] The use of standard norm-conserving pseudopotentials[48,49] avoids the computation of core electrons, smoothing at the same time the valence charge density. Basis functions consist of localized (numerical) pseudoatomic orbitals, projected on a real space grid to compute the Hartree potential and exchange correlation potentials matrix elements. For all atoms, basis sets of double plus polarization quality were employed, with a pseudoatomic orbital energy shift of 25 meV and a grid cutoff of 150 Ry. Calculations were performed using the generalized gradient approximation functional proposed by Perdew, Burke, and Ernzerhof.[50] The classical subsystem was treated using the parametrization from the AMBER force field. The frontier between the QM and MM portions of the system has been treated by the scaled position link atom method[51,52] adapted to the SIESTA code.[53]

Substrates IPP and DMAPP, the three magnesium atoms of the active site that coordinate the substrates, and one molecule of water, which coordinates the pyrophosphate group of DMAPP, a total of 52 atoms, were selected as the quantum subsystem (Figure 1). Two other more extended quantum subsystems were used, one with the side chain of Lys[202], a total of 66 atoms, and a second one including the side chains of Arg[(69,116)] for a total of 84 atoms. Link atoms have been used in the side chain of Lys[202] or Arg[(69,116)] to separate the QM-treated system from the backbone of the amino acids. The rest of the FPPS protein unit, together with water molecules, was treated classically. More technical details about the QM/MM implementation can be found elsewhere.[53]

The complex obtained from the molecular dynamics simulations was further relaxed by hybrid quantum−classical (QM/MM) geometry optimizations using a conjugate gradient algorithm. Magnesium atom positions were constrained during the optimizations. Only residues located less than 8 Å apart from the catalytic center were allowed to move freely in the QM/MM runs. We then computed the potential energy profiles using restrained energy minimizations along the selected reaction paths. For this purpose, an additional term is added to the potential energy according to $V(\xi) = k(\xi - \xi_0)^2$, where k is an adjustable force constant, ξ is the value of the reaction

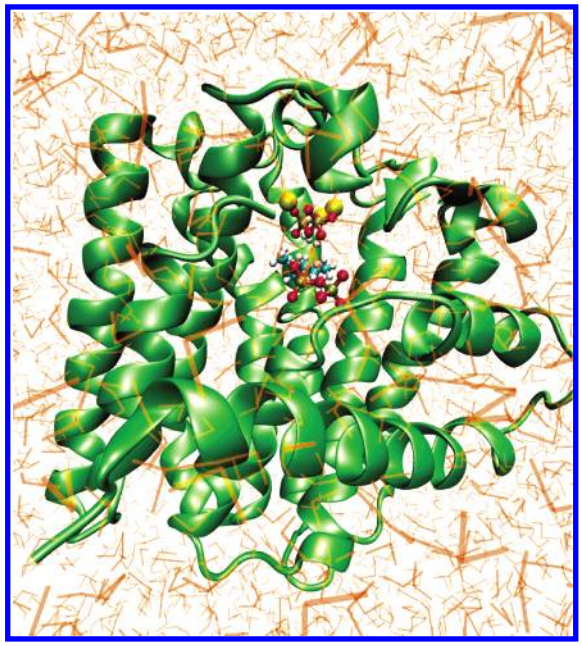

Figure 1. Representation of the FPPS enzyme in a sphere of water molecules. The nine helices of the fold are shown in ribbons mode. The atoms selected as the quantum subsystem are depicted in ball-and-stick mode: DMAPP (up), IPP (down), a water molecule, and the three Mg^{2+} ions. The image was generated with VMD (ref 57).

coordinate in the system particular configuration, and ξ_0 is the reaction coordinate desired value. Varying ξ_0, the system is forced to follow the minimum reaction path along the given coordinate. This method has been successfully applied in QM/MM reaction path calculations.

Results and Discussion

As a starting point for the simulations we used the X-ray structure of FPPS with DMAPP, IPP, and three Mg^{2+} atoms (PDB code 1RQJ).[8] We solvated the complex with a cap of explicit TIP3P[39] water molecules and relaxed the structure by a 100 ps of equilibration keeping the whole protein fixed, a subsequent 400 ps of unrestrained MD, and finally the system was cooled to 0 K. As quantum subsystem we selected IPP, DMAPP, and 3 Mg^{2+} ions present in the active site and one molecule of water, which coordinates the pyrophosphate group of DMAPP.

As stated above two main mechanisms were proposed for the farnesylation that is catalyzed by FPPS.[8,24,26,27] The first one involves the heterolytic cleavage of the C_1-O_7 bond of DMAPP that produces a cationic intermediate which then attacks the C_4 sp^2 carbon of IPP, and finally a hydrogen atom is transferred from the newly formed GPP to the leaving pyrophosphate group. The second one is a concerted mechanism, where the three previous steps occur together with only one transition state (TS) with a carbocationic character (Scheme 1). We thoroughly studied different mechanisms for the reaction by selecting different reaction coordinates. We found that the only feasible one involved the simultaneous rupture of the C_1-O_7 bond, the formation of the C_1-C_4 bond, and the transfer of the H_3 hydrogen to a negative pyrophosphate oxygen, O_6. As reaction coordinate (RC) we used the C_1-O_7 distance minus the C_1-C_4 distance ($RC = d(C_1-O_7) - d(C_1-C_4)$) (Scheme 1). The energy versus reaction coordinate profile is shown in Figure 2; the potential energy barrier turned out to be 26.4 kcal/mol. In Figures 3−5 snapshots of the reaction representing reactives, TS, and products are depicted.

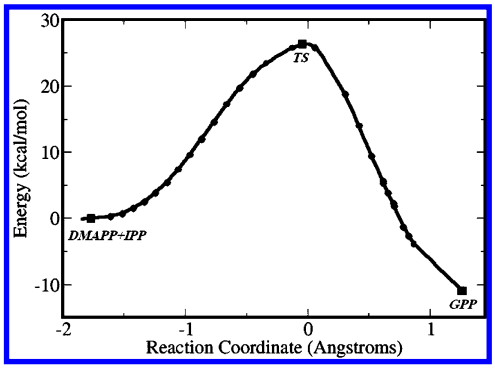

Figure 2. Energy vs reaction coordinate, the rupture of the C_1-O_7 bond, and the formation of the C_1-C_4 bond ($d(C_1-O_7) - d(C_1-C_4)$). In circles are the points in the reaction mechanism obtained by constrained minimization. The rectangles show the reactive, transition state, and product.

To test the possibility that important conserved amino acids involved in ligand binding were playing an important role in the reaction pathway or not, we also studied two other extended quantum subsystems, one with the side chain of Lys^{202} which is forming a hydrogen bond with the O_7 atom of DMAPP (Figure 3B) and the other with the side chains of $Arg^{(69,116)}$ which are involved in salt bridges with the pyrophosphate moiety of IPP and DMAPP (Figure 3B). There was a possibility that, as the reactives are strongly negatively charged and strong rearrangements occur during the reaction process, these amino acids could participate in the reaction by donating hydrogen atoms to the pyrophosphate moiety or that significant charge transfer could occur between them and the substrates. This possibility is excluded if these amino acids are not included in the QM subsystem. However, different reaction mechanisms were tested, and we found the same results as in the smaller system. The reaction occurs in one step with the same potential energy barrier as before, which suggests that these amino acids are important for binding and keeping the substrates in the correct conformation for the reaction to take place but are not specifically involved in the reaction mechanism, neither by accepting charge from the substrates nor by proton donation, as has been suggested.[54,55]

To better understand the reaction mechanism, relevant bond distances were followed (C_1-O_7, C_1-C_4, and C_5-H_3) as a function of the reaction coordinate (Figure 6). It can be seen that at the beginning of the reaction the distance between C_1-C_4 gets shorter (from 3.25 to 2.75 Å), while the C_1-O_7 is practically constant, mostly a movement between the two substrates. As the reaction follows, the breaking of the C_1-O_7 bond is simultaneous with the formation of the C_1-C_4 bond, while the H_3 hydrogen is still bound to the C_5 carbon. At the end of the reaction the H_3 hydrogen is transferred from the C_5 carbon to the O_6 oxygen. The most relevant geometrical parameters for reactive, TS, and product are summarized in Table 1.

As going from the reactive to the transition state the C_1 carbon adopts an sp^2 configuration (Figure 4) and acquires a carbocationic character, changing its Mulliken charge from 0.38 to 0.50 *e* (Table 1), the C_8 carbon also increases its Mulliken charge from 0.13 to 0.19 *e*, as expected if resonance of the double bond is considered. The O_7 oxygen gets polarized by a net increase in its negative Mulliken charge (Table 1), and the whole pyrophosphate moiety of DMAPP gains a total of −0.35 *e* at the TS. This may increase the basicity of this moiety and may favor the subsequent hydrogen abstraction from IPP. Interestingly, the IPP moiety has only slight structural changes at the

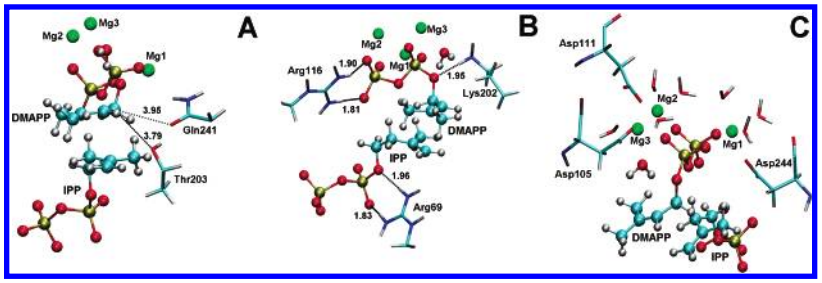

Figure 3. Three different views of the quantum subsystem in the reactive state. DMAPP, IPP, the three Mg^{2+} ions, and a water molecule are depicted in ball-and-stick mode. (A) Gln^{241} and Thr^{203} in bonds mode. (B) Side chains of $Arg^{(69,116)}$ and Lys^{202} included in the extended subsystems in bonds mode. (C) Aspartic amino acids and water molecules involved in magnesium binding in bonds mode.

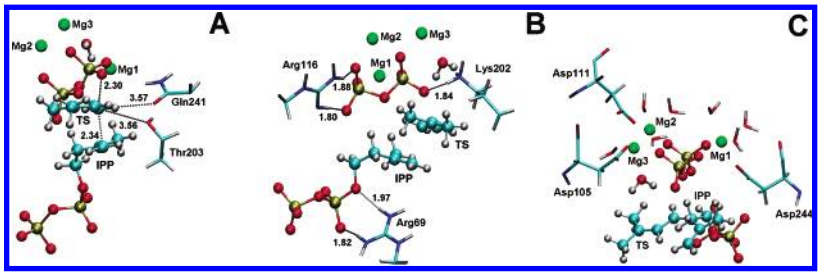

Figure 4. Three different views of the quantum subsystem in the transition state. Same rendering as Figure 3.

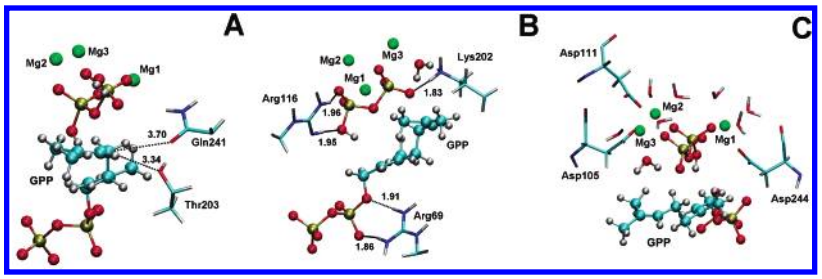

Figure 5. Three different views of the quantum subsystem in the product state. Same rendering as Figure 3.

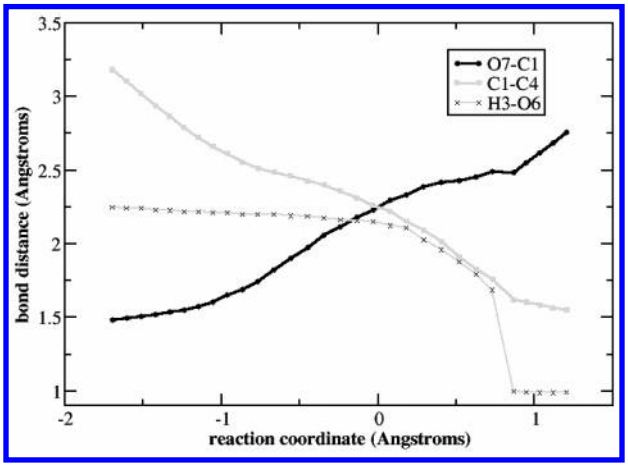

Figure 6. Bond distances (C_1-O_7, C_1-C_4, and C_5-H_3) as a function of the reaction coordinate.

TS state, and a small change in the charge distribution, gaining a total of 0.13 *e*; in this sense the C_1-C_4 bond is poorly formed (Figure 4). The water molecule included in the QM subsystem is making a hydrogen bond with the O_7 oxygen of DMAPP and changes its total charge during the reaction, going from -0.04 to -0.10 *e* at the TS, a charge transfer to the water that possibly stabilizes the TS. When GPP is formed, the C_1 carbon recuperates its sp^3 character, the whole aliphatic side chain becomes neutral, and the new double bond is formed (Table 1 and Figure 5). The H_3 is transferred to the pyrophosphate moiety gaining a total $+1$ *e* charge and the water molecule remains negative, -0.08 *e*, but with a minor value than before. The

TABLE 1: Selected Bond Distances (Å) and Charges (*e*) of Reactives, Transition State, and Products

	reactives	transition state	product
C_4-C_1	3.26	2.34	1.55
C_1-O_7	1.49	2.30	2.81
C_5-H_3	1.12	1.13	2.74
H_3-O_6	2.39	2.20	0.99
$C_{1\ DMAPP}$	sp^3	sp^2	sp^3
charge O_7	-0.25	-0.42	-0.36
charge C_1	0.38	0.50	0.35
total charge of H_2O	-0.04	-0.10	-0.08

charge of the Mg^{2+} cations does not change along the reaction, and there is no considerable charge transfer from DMAPP to them, suggesting that their primary role in the reaction may be to form a bridge between the enzyme and DMAPP which allows the substrate to bind in the proper conformation.

We evaluated the interaction between three amino acids, which have been proposed to be important in lowering the activation barrier.[8] It was believed that Lys^{202}, Thr^{203}, and Gln^{241} stabilized the carbocationic intermediate/TS by directing their dipoles toward the positive C_1 carbon.[8] When the TS is formed, the distance from the backbone carbonyl oxygen of Lys^{202}, the hydroxyl oxygen of Thr^{203}, and the terminal carbonyl of Gln^{241} to C_1 are 4.76, 3.56, and 3.57 Å, respectively (Figure 4A). To evaluate their role in stabilizing the TS, as these amino acids were considered part of the classical subsystem, we neglected the Coulombic interaction between them and the QM subsystem and recalculated the difference in energy between the reactive and the TS (Table 2). All three amino acids have positive

TABLE 2: Energy Stabilization

	potential energy barrier (kcal/mol)	relative stabilization energy (kcal/mol)
WT	26.3	0.0
s/Gln^{241} [a]	28.4	2.1
s/Thr^{203} [b]	27.9	1.5
s/Lys^{202} [c]	27.2	0.9

[a] For Gln^{241} the side chain amide group charge was made zero. [b] For Thr^{203} the side chain alcohol group charge was made zero. [c] For Lys^{202} the backbone carbonyl group charge was made zero.

stabilization energy; as expected, Lys^{202} has the least stabilization energy due to the longer distance to C_1, and Gln^{241} has the highest stabilization energy with 2.1 kcal/mol.

Conclusion

FPPS belongs to an important family of enzymes, isoprenyl diphosphate synthases, which are important for several biosynthetic pathways[1] and for the treatment of a variety of diseases.[4−6,9,15,16] Thus, understanding its mechanism of action is important per se and for the future development of new and more potent drugs. Recent crystallographic studies[8,15,19,20] have shown the characteristics of the active site that led to the proposal of different mechanisms. We have provided evidence that the mechanism is concerted with a TS that exhibits a carbocationic character. We have also established that the three positive amino acids (Lys^{202}, $Arg^{(69,116)}$), important for ligand binding, do not participate as charge acceptors or proton donors. Moreover, Mg^{2+} cations seem to have an important electrostatic role in the reaction, allowing DMAPP to stay in the proper conformation for the reaction to take place, but they are not involved in important charge transfer with the substrate during the reaction.

Nitrogen-containing bisphosphonates have been claimed as analogues of the transition state/carbocationic intermediate as an explanation for their strong activity; our results support this hypothesis as the transition state has a strong localized positive charge in the C_1 carbon. However, one would have expected a greater interaction of the TS with the enzyme polar amino acids that are surrounding the C_1 carbon, and in this sense it is likely that other effects as ligand hydration/dehydration effects may play an important role,[56] which may explain also the strong activity observed in bisphosphonates lacking the positive charge.

Acknowledgment. We acknowledge Dr. S. Szajnman, Dr. Rodriguez, and Dr. Estrin for fruitful discussions. A.G.T. acknowledges financial support from the PEW charitable trust and NIH. L. Sigman and V. Sanchez are fellows from the Universidad de Buenos Aires.

References and Notes

(1) Glomset, J. A.; Gelb, M. H.; Farnsworth, C. C. Prenyl proteins in eukaryotic cells: a new type of membrane anchor. *Trends Biochem. Sci.* **1990**, *15* (4), 139−142.

(2) Ashby, M. N.; Edwards, P. A. Identification and regulation of a rat liver cDNA encoding farnesyl pyrophosphate synthetase. *J. Biol. Chem.* **1989**, *264* (1), 635−640.

(3) Urbina, J. A.; Moreno, B.; Vierkotter, S.; Oldfield, E.; Payares, G.; Sanoja, C.; Bailey, B. N.; Yan, W.; Scott, D. A.; Moreno, S. N.; Docampo, R. *Trypanosoma cruzi* contains major pyrophosphate stores, and its growth in vitro and in vivo is blocked by pyrophosphate analogues. *J. Biol. Chem.* **1999**, *274* (47), 33609−33615.

(4) Dunford, J. E.; Thompson, K.; Coxon, F. P.; Luckman, S. P.; Hahn, F. M.; Poulter, C. D.; Ebetino, F. H.; Rogers, M. J. Structure−activity relationships for inhibition of farnesyl diphosphate synthase in vitro and inhibition of bone resorption in vivo by nitrogen-containing bisphosphonates. *J. Pharmacol. Exp. Ther.* **2001**, *296* (2), 235−242.

(5) Sanders, J. M.; Song, Y.; Chan, J. M.; Zhang, Y.; Jennings, S.; Kosztowski, T.; Odeh, S.; Flessner, R.; Schwerdtfeger, C.; Kotsikorou, E.; Meints, G. A.; Gomez, A. O.; Gonzalez-Pacanowska, D.; Raker, A. M.; Wang, H.; van Beek, E. R.; Papapoulos, S. E.; Morita, C. T.; Oldfield, E. Pyridinium-1-yl bisphosphonates are potent inhibitors of farnesyl diphosphate synthase and bone resorption. *J. Med. Chem.* **2005**, *48* (8), 2957−2963.

(6) Ling, Y.; Sahota, G.; Odeh, S.; Chan, J. M.; Araujo, F. G.; Moreno, S. N.; Oldfield, E. Bisphosphonate inhibitors of *Toxoplasma gondi* growth: in vitro, QSAR, and in vivo investigations. *J. Med. Chem.* **2005**, *48* (9), 3130−3140.

(7) Cheng, F.; Oldfield, E. Inhibition of isoprene biosynthesis pathway enzymes by phosphonates, bisphosphonates, and diphosphates. *J. Med. Chem.* **2004**, *47* (21), 5149−5158.

(8) Hosfield, D. J.; Zhang, Y.; Dougan, D. R.; Broun, A.; Tari, L. W.; Swanson, R. V.; Finn, J. Structural basis for bisphosphonate-mediated inhibition of isoprenoid biosynthesis. *J. Biol. Chem.* **2004**, *279* (10), 8526−8529.

(9) Szajnman, S. H.; Ravaschino, E. L.; Docampo, R.; Rodriguez, J. B. Synthesis and biological evaluation of 1-amino-1,1-bisphosphonates derived from fatty acids against *Trypanosoma cruzi* targeting farnesyl pyrophosphate synthase. *Bioorg. Med. Chem. Lett.* **2005**, *15*, 4685−4690.

(10) van Beek, E. R.; Cohen, L. H.; Leroy, I. M.; Ebetino, F. H.; Lowik, C. W.; Papapoulos, S. E. Differentiating the mechanisms of antiresorptive action of nitrogen containing bisphosphonates. *Bone* **2003**, *33* (5), 805−811.

(11) van Beek, E. R.; Lowik, C. W.; Papapoulos, S. E. Bisphosphonates suppress bone resorption by a direct effect on early osteoclast precursors without affecting the osteoclastogenic capacity of osteogenic cells: the role of protein geranylgeranylation in the action of nitrogen-containing bisphosphonates on osteoclast precursors. *Bone* **2002**, *30* (1), 64−70.

(12) Cinque, G. M.; Szajnman, S. H.; Zhong, L.; Docampo, R.; Schvartzapel, A. J.; Rodriguez, J. B.; Gros, E. G. Structure−activity relationship of new growth inhibitors of *Trypanosoma cruzi*. *J. Med. Chem.* **1998**, *41*, 1 (9), 1540−1554.

(13) Garzoni, L. R.; Waghabi, M. C.; Baptista, M. M.; de Castro, S. L.; Meirelles, M. N.; Britto, C. C.; Docampo, R.; Oldfield, E.; Urbina, J. A. Antiparasitic activity of risedronate in a murine model of acute Chagas' disease. *Int. J. Antimicrob. Agents* **2004**, *23* (3), 286−290.

(14) Garzoni, L. R.; Caldera, A.; Meirelles, M. N.; de Castro, S. L.; Docampo, R.; Meints, G. A.; Oldfield, E.; Urbina, J. A. Selective in vitro effects of the farnesyl pyrophosphate synthase inhibitor risedronate on *Trypanosoma cruzi*. *Int. J. Antimicrob. Agents* **2004**, *23* (3), 273−285.

(15) Montalvetti, A.; Bailey, B. N.; Martin, M. B.; Severin, G. W.; Oldfield, E.; Docampo, R. Bisphosphonates are potent inhibitors of *Trypanosoma cruzi* farnesyl pyrophosphate synthase. *J. Biol. Chem.* **2001**, *276* (36), 33930−33937.

(16) Szajnman, S. H.; Montalvetti, A.; Wang, Y.; Docampo, R.; Rodriguez, J. B. Bisphosphonates derived from fatty acids are potent inhibitors of *Trypanosoma cruzi* farnesyl pyrophosphate synthase. *Bioorg. Med. Chem. Lett.* **2003**, *13* (19), 3231−3235.

(17) Urbina, J. A.; Docampo, R. Specific chemotherapy of Chagas disease: controversies and advances. *Trends Parasitol.* **2003**, *19* (11), 495−501.

(18) Miles, M. A.; Feliciangeli, M. D.; de Arias, A. R. American trypanosomiasis (Chagas' disease) and the role of molecular epidemiology in guiding control strategies. *Br. Med. J.* **2003**, *326* (7404), 1444−1448.

(19) Tarshis, L. C.; Yan, M.; Poulter, C. D.; Sacchettini, J. C. Crystal structure of recombinant farnesyl diphosphate synthase at 2.6-A resolution. *Biochemistry* **1994**, *33*, (36), 10871−10877.

(20) Tarshis, L. C.; Proteau, P. J.; Kellogg, B. A.; Sacchettini, J. C.; Poulter, C. D. Regulation of product chain length by isoprenyl diphosphate synthases. *Proc. Natl. Acad. Sci. U.S.A.* **1996**, *93* (26), 15018−15023.

(21) Kavanagh, K. L.; Guo, K.; Dunford, J. E.; Wu, X.; Knapp, S.; Ebetino, F. H.; Rogers, M. J.; Russell, R. G.; Oppermann, U. The molecular mechanism of nitrogen-containing bisphosphonates as antiosteoporosis drugs. *Proc. Natl. Acad. Sci. U.S.A.* **2006**, *103* (20), 7829−7834.

(22) Phan, R. M.; Poulter, C. D. Synthesis of (*S*)-isoprenoid thiodiphosphates as substrates and inhibitors. *J. Org. Chem.* **2001**, *66* (20), 6705−6710.

(23) Sigman, L.; Sanchez, V. M.; Turjanski, A. G. Characterization of the farnesyl pyrophosphate synthase of *Trypanosoma cruzi* by homology modeling and molecular dynamics. *J. Mol. Modell.*, in press.

(24) Gabelli, S. B.; McLellan, J. S.; Montalvetti, A.; Oldfield, E.; Docampo, R.; Amzel, L. M. Structure and mechanism of the farnesyl diphosphate synthase from *Trypanosoma cruzi*: implications for drug design. *Proteins* **2006**, *62* (1), 80−88.

(25) Martin, M. B.; Arnold, W.; Heath, H. T., III; Urbina, J. A.; Oldfield, E. Nitrogen-containing bisphosphonates as carbocation transition state analogues for isoprenoid biosynthesis. *Biochem. Biophys. Res. Commun.* **1999**, *263* (3), 754−758.

(26) Cornforth, J. W. Olefin alkylation in biosynthesis. *Angew. Chem., Int. Ed Engl.* **1968**, *7* (12), 903−911.

(27) Rilling, H. C.; Bloch, K. On the mechanism of squalene biogenesis from mevalonic acid. *J. Biol. Chem.* **1959**, *234* (6), 1424−1432.

(28) Mulholland, A. J.; Grant, G. H.; Richards, W. G. Computer modelling of enzyme catalysed reaction mechanisms. *Protein Eng.* **1993**, *6* (2), 133−147.

(29) Friesner, R. A.; Guallar, V. Ab initio quantum chemical and mixed quantum mechanics/molecular mechanics (QM/MM) methods for studying enzymatic catalysis. *Annu. Rev. Phys. Chem.* **2005**, *56*, 389−427.

(30) Marti, M. A.; Crespo, A.; Capece, L.; Boechi, L.; Bikiel, D. E.; Scherlis, D. A.; Estrin, D. A. Dioxygen affinity in heme proteins investigated by computer simulation. *J. Inorg. Biochem.* **2006**, *100*, 761−770.

(31) Fernandez, M. L.; Marti, M. A.; Crespo, A.; Estrin, D. A. Proximal effects in the modulation of nitric oxide synthase reactivity: a QM−MM study. *J. Biol. Inorg. Chem.* **2005**, *10* (6), 595−604.

(32) Crespo, A.; Marti, M. A.; Kalko, S. G.; Morreale, A.; Orozco, M.; Gelpi, J. L.; Luque, F. J.; Estrin, D. A. Theoretical study of the truncated hemoglobin HbN: exploring the molecular basis of the NO detoxification mechanism. *J. Am. Chem. Soc.* **2005**, *127* (12), 4433−4444.

(33) Marti, M. A.; Scherlis, D. A.; Doctorovich, F. A.; Ordejon, P.; Estrin, D. A. Modulation of the NO trans effect in heme proteins: implications for the activation of soluble guanylate cyclase. *J. Biol. Inorg. Chem.* **2003**, *8* (6), 595−600.

(34) Zhang, Y.; Kua, J.; McCammon, J. A. Role of the catalytic triad and oxyanion hole in acetylcholinesterase catalysis: an ab initio QM/MM study. *J. Am. Chem. Soc.* **2002**, *124* (35), 10572−10577.

(35) Puig, E.; Garcia-Viloca, M.; Gonzalez-Lafont, A.; Lluch, J. M. On the ionization state of the substrate in the active site of glutamate racemase. A QM/MM study about the importance of being zwitterionic. *J. Phys. Chem. A* **2006**, *110* (2), 717−725.

(36) Garcia-Viloca, M.; Gonzalez-Lafont, A.; Lluch, J. M. A QM/MM study of the racemization of vinylglycolate catalyzed by mandelate racemase enzyme. *J. Am. Chem. Soc.* **2001**, *123* (4), 709−721.

(37) Dinner, A. R.; Blackburn, G. M.; Karplus, M. Uracil−DNA glycosylase acts by substrate autocatalysis. *Nature* **2001**, *413* (6857), 752−755.

(38) Berman, H. M.; Battistuz, T.; Bhat, T. N.; Bluhm, W. F.; Bourne, P. E.; Burkhardt, K.; Feng, Z.; Gilliland, G. L.; Iype, L.; Jain, S.; Fagan, P.; Marvin, J.; Padilla, D.; Ravichandran, V.; Schneider, B.; Thanki, N.; Weissig, H.; Westbrook, J. D.; Zardecki, C. The protein data bank. *Acta Crystallogr., Sect D* **2002**, *58* (Part 6, No. 1), 899−907.

(39) Jorgensen, W. L.; Chandrasekhar, J.; Madura, J. D.; Impey, R. W.; Klein, M. L. Comparison of simple potential functions for simulating liquid water. *J. Chem. Phys.* **1983**, *79* (2), 926−935.

(40) Kale, L.; Skeel, R.; Bhandarkar, M.; Brunner, R.; Gursoy, A.; Krawetz, N.; Phillips, J.; Shinozaki, A.; Varadarajan, K.; Schulten, K. NAMD2: Greater scalability for parallel molecular dynamics. *J. Comput. Phys.* **1999**, *151* (1), 283−312.

(41) Wang, J. M.; Cieplak, P.; Kollman, P. A. How well does a restrained electrostatic potential (RESP) model perform in calculating conformational energies of organic and biological molecules? *J. Comput. Chem.* **2000**, *21* (12), 1049−1074.

(42) *Amber 7*; University of California: San Francisco, CA, 2002.

(43) Breneman, C. M.; Wiberg, K. B. Determining atom-centered monopoles from molecular electrostatic potentials—the need for high sampling density in formamide conformational-analysis. *J. Comput. Chem.* **1990**, *11* (3), 361−373.

(44) *Gaussian 98*, rev. A7.; Gaussian, Inc.: Pittsburgh, PA, 1998.

(45) Cornell, W. D.; Cieplak, P.; Bayly, C. I.; Gould, I. R.; Merz, K. M.; Ferguson, D. M.; Spellmeyer, D. C.; Fox, T.; Caldwell, J. W.; Kollman, P. A. A 2nd generation force-field for the simulation of proteins, nucleic acids, and organic molecules. *J. Am. Chem. Soc.* **1995**, *117* (19), 5179−5197.

(46) Berendsen, H. J. C.; Postma, J. P. M.; Vangunsteren, W. F.; Dinola, A.; Haak, J. R. Molecular-dynamics with coupling to an external bath. *J. Chem. Phys.* **1984**, *81* (8), 3684−3690.

(47) Soler, J. M.; Artacho, E.; Gale, J. D.; Garcia, A.; Junquera, J.; Ordejon, P.; Sanchez-Portal, D. The SIESTA method for ab initio order-N materials simulation. *J. Phys.: Condens. Matter* **2002**, *14* (11), 2745−2779.

(48) Troullier, N.; Martins, J. L. Efficient pseudopotentials for plane-wave calculations. 2. Operators for fast iterative diagonalization. *Phys. Rev. B* **1991**, *43* (11), 8861−8869.

(49) Troullier, N.; Martins, J. L. Efficient pseudopotentials for plane-wave calculations. *Phys. Rev. B* **1991**, *43* (3), 1993−2006.

(50) Perdew, J. P.; Burke, K.; Ernzerhof, M. Generalized gradient approximation made simple. *Phys. Rev. Lett.* **1996**, *77* (18), 3865−3868.

(51) Rovira, C.; Schulze, B.; Eichinger, M.; Evanseck, J. D.; Parrinello, M. Influence of the heme pocket conformation on the structure and vibrations of the Fe−CO bond in myoglobin: a QM/MM density functional study. *Biophys. J.* **2001**, *81* (1), 435−445.

(52) Eichinger, M.; Tavan, P.; Hutter, J.; Parrinello, M. A hybrid method for solutes in complex solvents: Density functional theory combined with empirical force fields. *J. Chem. Phys.* **1999**, *110* (21), 10452−10467.

(53) Crespo, A.; Scherlis, D. A.; Marti, M. A.; Ordejon, P.; Roitberg, A. E.; Estrin, D. A. A DFT-based QM−MM approach designed for the treatment of large molecular systems: Application to chorismate mutase. *J. Phys. Chem. B* **2003**, *107* (49), 13728−13736.

(54) Song, L.; Poulter, C. D. Yeast farnesyl-diphosphate synthase: site-directed mutagenesis of residues in highly conserved prenyltransferase domains I and II. *Proc. Natl. Acad. Sci. U.S.A.* **1994**, *91* (8), 3044−3048.

(55) Koyama, T.; Tajima, M.; Sano, H.; Doi, T.; Koike-Takeshita, A.; Obata, S.; Nishino, T.; Ogura, K. Identification of significant residues in the substrate binding site of *Bacillus stearothermophilus* farnesyl diphosphate synthase. *Biochemistry* **1996**, *35*, (29), 9533−9538.

(56) Yin, F.; Cao, R.; Goddard, A.; Zhang, Y.; Oldfield, E. Enthalpy versus entropy-driven binding of bisphosphonates to farnesyl diphosphate synthase. *J. Am. Chem. Soc.* **2006**, *128* (11), 3524−3525.

(57) Humphrey, W.; Dalke, A.; Schulten, K. VMD: visual molecular dynamics. *J. Mol. Graphics* **1996**, *14* (1), 33−38.